



Critical thickness for itinerant ferromagnetism in ultrathin films of SrRuO₃

Jing Xia,^{1,2} W. Siemons,^{1,3} G. Koster,^{1,3} M. R. Beasley,^{1,4} and A. Kapitulnik^{1,2,4}

¹*Geballe Laboratory for Advanced Materials, Stanford University, Stanford, California 94305, USA*

²*Department of Physics, Stanford University, Stanford, California 94305, USA*

³*Faculty of Science and Technology and MESA+ Institute for Nanotechnology, University of Twente, P.O. Box 217, 7500 AE, Enschede, The Netherlands*

⁴*Department of Applied Physics, Stanford University, Stanford, California 94305, USA*

(Received 16 March 2009; published 16 April 2009)

Ultrathin films of the itinerant ferromagnet SrRuO₃ were studied using the transport and magneto-optic polar Kerr effect. We find that below 4 monolayers, the films become insulating and their magnetic character changes as they lose their simple ferromagnetic behavior. We observe a strong reduction in the magnetic moment which for 3 monolayers and below lies in the plane of the film. Exchange-bias behavior is observed below the critical thickness and may point to induced antiferromagnetism in contact with ferromagnetic regions.

DOI: [10.1103/PhysRevB.79.140407](https://doi.org/10.1103/PhysRevB.79.140407)

PACS number(s): 75.70.-i, 75.30.Cr, 75.30.Gw, 75.60.-d

SrRuO₃ is an itinerant ferromagnet with an orthorhombically distorted cubic perovskite structure, exhibiting a transition to a ferromagnetic (FM) state at $T_c \sim 160$ K that was shown to be dominated by transverse fluctuations of robust local moments of size $\sim 1.6\mu_B$,¹ the largest of any 4d ferromagnet. While the high-temperature paramagnetic phase is dominated by a “bad metal” behavior in the limit of $k_F\ell \sim 1$ (Ref. 2) suggesting that Fermi-liquid theory may not be valid, the observation of quantum oscillations in the resistivity of high-quality thin films of SrRuO₃ demonstrated that the ground state of this system is a Fermi liquid.³ At the same time, the degree of electron correlation in SrRuO₃ has been found to be a strong function of ruthenium deficiency.⁴ To understand the contrast in the behavior of SrRuO₃ between high and low temperatures, appropriate perturbations, such as disorder and reduced dimensionality, may be used that directly disturb the magnetic and transport properties of the system. Indeed, recent studies of the thickness dependence of the transport and electronic structure of SrRuO₃ films^{5,6} concluded that a metal-insulator transition (MIT) occurs in these films at a critical film thickness of 4 or 5 monolayers (MLs), depending on the disorder. However, the reported islandlike microstructure showing coalescence of three-dimensional patches and the inability to study the nature of the magnetism hinder any possible understanding of the observed transition. Since this may be an example of the interplay between itinerancy, ferromagnetism, disorder and dimensionality, better films growth, and a more direct probe of magnetism are needed to establish the important ingredients of the physics involved.

In this Rapid Communication, we present results on the MIT in ultrathin SrRuO₃ films and their associated magnetic properties. We show that in homogeneous films of SrRuO₃, a MIT occurs at a critical thickness below 4 ML. While T_c drops rapidly below ~ 10 ML, the size of the moment remains unchanged from its $1.6\mu_B$ in thick films,¹ and the easy axis which has been closer to normal for thick films becomes even more normal. However, below the critical thickness the easy axis of the moment plummets to the plane of the film and an exchange-bias (EB) behavior emerges, suggesting the existence of antiferromagnetic (AF) regions (or layers) that

interact with the remaining ferromagnetic regions (or layers). Transport measurements reveal an increase in the resistance with decreasing thickness. At 4 ML, the extrapolated low-temperature sheet resistance is of order ~ 7 k Ω , jumping up 8 orders of magnitude in 3 ML films.

SrRuO₃ samples used in our experiment were grown by pulsed laser deposition (PLD). The samples were grown in a vacuum chamber with a background pressure of 10^{-7} Torr. A 248-nm-wavelength KrF excimer laser was employed with typical pulse lengths of 20–30 ns. The energy density on the target is kept at approximately 2.1 J/cm². All films were grown on TiO₂ terminated SrTiO₃ substrates,⁷ at 700 C, with a laser repetition rate of 4 Hz. We have calibrated the deposition rate multiple times throughout the process by performing x-ray reflectivity on thicker samples. The thickness of the films range from 2 to 25 ML, each with an uncertainty of only a few laser pulses, which is equivalent to a very small fraction of a 1 ML (approximately 20 pulses per 1 ML).

Atomic force microscope (AFM) images (Fig. 1) taken immediately following deposition indicate that between 2 and 7 ML, SrRuO₃ films show homogeneous coverage of the substrate, with two-dimensional stripe-shaped steps following the ($\sim 0.2^\circ$) miscut of the substrate. These two-

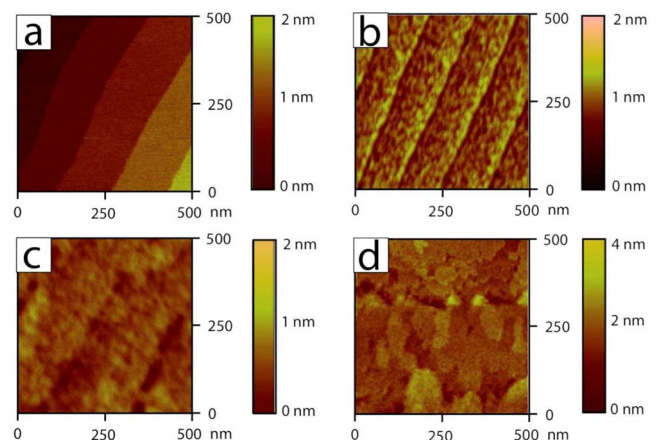


FIG. 1. (Color online) AFM images of (a) SrTiO₃ substrate before deposition, (b) 2 ML, (c) 5 ML, and (d) 9 ML (see text).

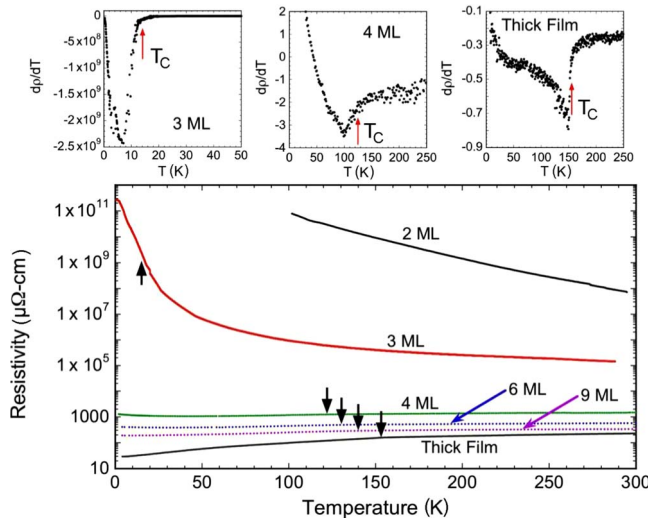


FIG. 2. (Color online) Resistivity data of SrRuO₃ films. Arrows point to the location of the ferromagnetic transition determined from the derivative of the resistivity (see, e.g., top panels for 3 ML, 4 ML, and thick film derivatives).

dimensional steps are 1 ML in height and are typically 100 nm in width. Moreover, unlike previous reports,^{6,8} no three-dimensional island growth was observed, indicating an atomically smooth surface and single domain structure in these films. The observed steplike growth seems to fade at thicknesses above 9 ML as the steps mostly coalesce, suggesting a transition from a growth mode of two-dimensional layer by layer to a step flow mode, in agreement with earlier reports.⁹

Figure 2 shows the resistivity of the films through the transition measured from room temperature down to 4.2 K. The ferromagnetic transition was noticeable in all films of 4 ML and above; however the transition becomes broad and difficult to determine for the very thin films. We note that while the extrapolated low-temperature sheet resistance of the 4 ML film is of order ~ 7 k Ω , the low-temperature resistance of the 3 ML film increases more than 8 orders of magnitude, much higher than the quantum of resistance for two dimensions of $h/e^2 \sim 26$ k Ω . Thus it is clear that a metal-insulator transition has occurred in between these two thicknesses.

The magnetic properties of the films were determined from Polar Kerr effect (PKE) measurements, which is only sensitive to the out-of-plane component of the magnetization.¹⁰ While in general for thin-films magnetism the Kerr signal is large,¹⁰ for ultrathin films (approaching 1 ML) of weak ferromagnets—especially deposited on strongly birefringent substrates—the signal may be difficult to resolve. In our case, SrRuO₃ films are deposited on miscut substrates of SrTiO₃ which are very strongly linearly birefringent. To overcome the above difficulties, we have used a zero-area-loop Sagnac interferometer.¹¹ This design is based on a Sagnac loop in which two counter-propagating beams with opposite circular polarization reflect from the sample while completing a Sagnac loop. This design which was introduced by Xia *et al.*¹¹ is capable of measuring time-reversal-symmetry-breaking effects with a shot-noise limited

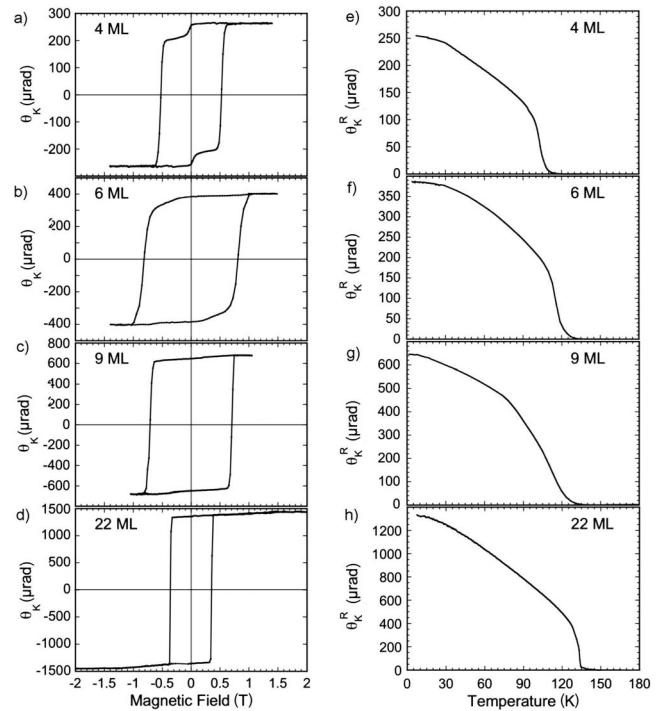


FIG. 3. Panels (a)–(d): PKE hysteresis loop for SrRuO₃ films of different thickness taken at 4 K, with magnetic field applied perpendicular to the plane of the film. Panels (e)–(h): temperature dependence of the remanent PKE signal measured at zero magnetic field during warmup, after a positive saturation magnetic field was turned off at the lowest temperature.

sensitivity of 100 nrad/ $\sqrt{\text{Hz}}$ at a power of 10 μW , while being completely immune to any reciprocal effects in the sample.¹² For the results reported in this Rapid Communication, we used a normal-incidence configuration, measuring at a wavelength of 1550 nm with a beam focused on the sample to a spot size of 3 μm and in the temperature range of 0.3 K to room temperature. Since the optical penetration depth at the used frequency is of order 200 nm, while the thickest sample used was only 8.8 nm, the signal measured—to a very good approximation—was simply proportional to the area density of the magnetic moment.¹⁰

Figure 3 shows the evolution of the PKE measured on the samples from 4 to 22 ML thick samples. Hysteresis loops were obtained by recording the Kerr signal at the lowest temperature (typically 0.4 K) while ramping an out-of-plane magnetic field and then subtracting the linear paramagnetic response from the SrTiO₃ substrate and diamagnetic response from the optical components in the fringing magnetic field. After the magnetic field was turned off, the PKE was measured as a function of temperature while the films were warmed to room temperature. This allowed the determination of the Curie temperature T_c and the angle of the easy axis.

The temperature-dependent remanent-Kerr effect of the 2 and 3 ML films did not show any ferromagnetic transition down to 0.4 K to a resolution of ± 0.2 μrad . However, we suggest that the magnetic transition may be deduced from the resistivity data that show sharp upturn in the resistivity of the 3 ML film below ~ 25 K (Fig. 2). The resistivity of the 2ML film could not be measured below 100 K due to the large

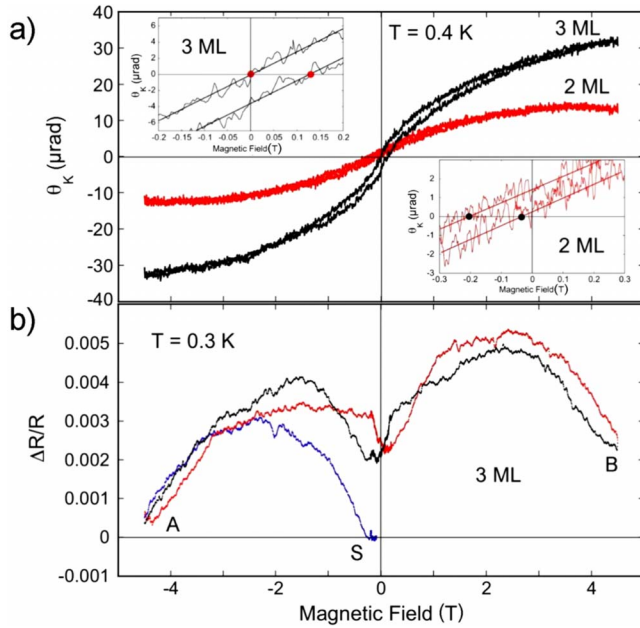


FIG. 4. (Color online) (a) Hysteresis loop for the 2 and 3 ML samples. Insets show the region near the origin where thick dots mark the crossing of the field axis. Here, the 3 ML is biased to the right and the 2 ML is biased to the left. (b) Magnetoresistance for the 3 ML sample. Loop starts at S, continues to A, then B, and ends at A. Subsequent loops trace the A-B-A loop.

resistance. Magnetization curves of 2 and 3 ML films at 0.4 K are shown in Fig. 4(a). These were obtained by first cooling in a field then performing a hysteresis loop followed by a subtraction of the (diamagnetic) contribution of the fiber strand in the magnet. The S shape and finite opening of both curves indicate that the low-temperature phase of these films has ferromagnetic component with moments that lie entirely in the plane of the film. The open loops are nonsymmetric with respect to zero field. The 3ML sample was cooled in a -5 kOe field and its low-temperature hysteresis loop is biased toward positive field, while the 2ML sample was cooled through in a $+5$ kOe field and its hysteresis loop is biased toward negative field. This behavior is reminiscent of the exchange-bias effect.¹³ EB phenomena originate at the interface of FM and AF regions, where uncompensated AF moments result in a bias magnetic field, causing the hysteresis loop of the FM to be shifted away from the origin.¹³ The hypotheses of both remanent in-plane ferromagnetism and EB are further supported by magnetoresistance (MR) measurements at 0.3 K shown in Fig. 4(b). We note that the maximum MR observed is $\Delta R/R \sim 0.005$, a very small effect when compared to the spin-scattering-dominated MIT.

The first sharp hysteresis loop is obtained for the 4 ML sample [Fig. 3(a)], pointing to ferromagnetism with an almost perpendicular moment.¹⁴ Turning off the magnetic field, a remanent signal is observed [$\theta_K^R(T)$] that disappears at T_c [Fig. 3(e)]. Similar data for other samples are given in Fig. 5 where we show the thickness dependence of the saturation Kerr signal [$\theta_K^S(T)$, which is determined as the highest point of the hysteresis loop in Fig. 3], the T_c of the layers, and the variation in the easy axis for all ferromagnetic films.

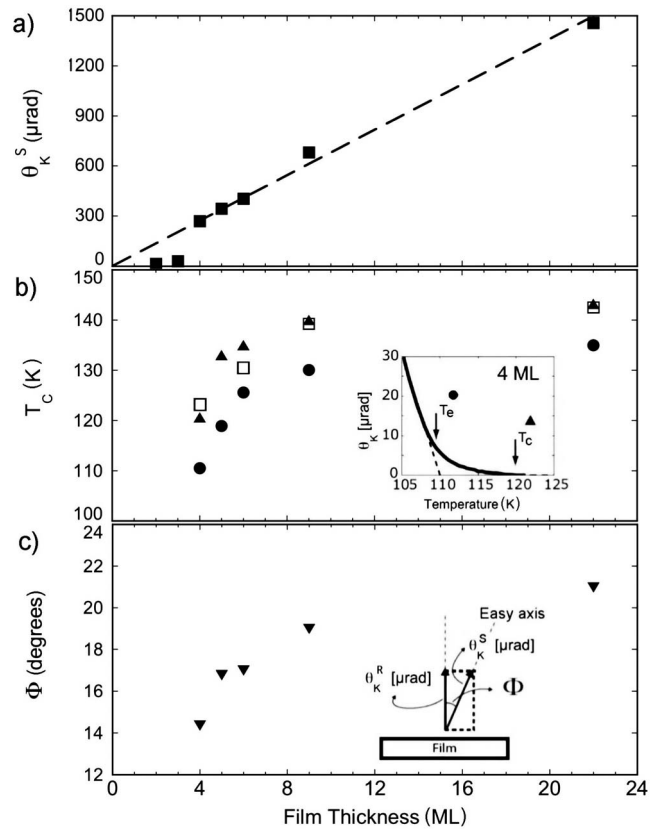


FIG. 5. Thickness dependencies of (a) saturated Kerr signal (■) at the lowest temperature; (b) Curie temperature T_c (▲), extrapolated Curie temperature T_e (●), and resistivity anomaly (□); and (c) the angle Φ (▼) between film normal and magnetic easy axis at the lowest temperature. Dashed line in (a) is the linear fit of the data point between 4 and 22 ML. Inset in (b) shows how T_c and T_e are determined.

Figure 5(a) shows that the saturated Kerr signal is proportional to the film thickness from the thick (22 ML) down to the thinnest samples (4 ML), extrapolating to zero thickness. Since we argued that all these films are in the very thin limit compared to the penetration depth of the light, this result clearly shows that the thick film moment ($\sim 1.6\mu_B$) does not change and that all the layers are ferromagnetic. Below 4 ML the saturation Kerr signal plummets, indicating a much smaller moment of $\sim 0.2\mu_B$.

Figure 5(b) shows the thickness dependence of T_c . To determine the temperature above which no ferromagnetism is observed, we magnified the region near the transition as shown in the inset of Fig. 5(b). While in general the magnetization vanishes at T_c with an exponent smaller than unity, the domain structure and reorientation in films may result in an apparent lower transition temperature (T_e).¹⁵ We therefore define two critical temperatures as shown in the inset and plot both in Fig. 5(b). We note that it is T_c (the temperature at which the Kerr signal vanishes), which smoothly extrapolates to the thick films limit and therefore to previously published data on three-dimensional SrRuO₃ films.¹⁶ Both T_e and T_c cannot be measured below 4 ML. We note that the anomaly in the resistivity measured by taking the derivative of the resistivity curves agrees with T_c for the very thin films

and continues toward the thick films limit as expected.^{16,17}

To determine the magnetic anisotropy angle, we calculate $\Phi = \cos^{-1}(\theta_K^R / \theta_K^S)$. This is plotted in Fig. 5(c). It was previously found that for high-quality epitaxial thick films and at low temperatures $\Phi \sim 30^\circ$.^{2,16} In Fig. 5(c) we show that Φ decreases from 22° in the case of 22 ML film to 14° in 4 ML film. Thus, the fact that below 4 ML the moment is almost entirely in the plane (Fig. 4), hence going in the complete opposite way to the trend we found above, is just another confirmation that a phase transition occurred between 3 and 4 monolayers.

In summary, we find that below 4 monolayers, otherwise metallic and ferromagnetic SrRuO₃ films grown on SrTiO₃ become insulating, and an AF layer appears with the moment in the plane of the films. Since both 3 and 2 ML films show an exchange-bias behavior, it is reasonable to assume that the AF layer emerges at the interface with the substrate and in contact with the FM layers above it. While previous simple theoretical investigations of SrRuO₃—including correlations—were unable to reproduce the experimentally observed MIT and disappearance of ferromagnetism,¹⁸ these results point to a possible resolution of the puzzle.

In a recent paper, Mahadevan *et al.*¹⁹ found that the SrTiO₃ substrate plays a crucial role in predicting the properties of ultrathin SrRuO₃ films. In such films, the substrate

induces structural distortions in the films and together with electron correlations it brings about crystal-field anisotropies very different from the bulk of SrRuO₃, inducing an insulating phase that is accompanied by the occurrence of antiferromagnetism in the otherwise metallic ferromagnetic phase. It is also expected that the increased disorder in the very thin films only helps in pinning this insulating phase. We therefore led to conclude that the recovery from the bottom antiferromagnetic layer to bulk itinerant ferromagnetism happens within the next two layers in which both antiferromagnetism and ferromagnetism exist as is evident from the observed exchange-bias behavior. The strong reduction in the moment from ~ 1.6 to $\sim 0.2\mu_B$ may further indicate strong changes in oxygen hybridization in the very thin films²⁰ or a possible proximity to a quantum critical point in which coupling to fluctuations causes the reduction in the moment.

Discussions with L. Klein and P. Mahadevan are greatly acknowledged. Fabrication of the Sagnac system was supported by Stanford's Center for Probing the Nanoscale, NSF NSEC under Grant No. 0425897. Work at Stanford was supported by the Department of Energy under Grant DE-AC02-76SF00515.

-
- ¹J. S. Dodge, E. Kulatov, L. Klein, C. H. Ahn, J. W. Reiner, L. Miéville, T. H. Geballe, M. R. Beasley, A. Kapitulnik, H. Ohta, Yu. Uspenskii, and S. Halilov, *Phys. Rev. B* **60**, R6987 (1999).
- ²L. Klein, J. S. Dodge, C. H. Ahn, G. J. Snyder, T. H. Geballe, M. R. Beasley, and A. Kapitulnik, *Phys. Rev. Lett.* **77**, 2774 (1996).
- ³A. P. Mackenzie, J. W. Reiner, A. W. Tyler, L. M. Galvin, S. R. Julian, M. R. Beasley, T. H. Geballe, and A. Kapitulnik, *Phys. Rev. B* **58**, R13318 (1998).
- ⁴W. Siemons, G. Koster, A. Vailionis, H. Yamamoto, D. H. A. Blank, and M. R. Beasley, *Phys. Rev. B* **76**, 075126 (2007).
- ⁵G. Herranz, B. Martinez, J. Fontcuberta, F. Sanchez, C. Ferrater, M. V. Garcia-Cuenca, and M. Varela, *Phys. Rev. B* **67**, 174423 (2003).
- ⁶D. Toyota, I. Ohkubo, H. Kumigashira, M. Oshima, T. Ohnishi, M. Lippmaa, M. Takizawa, A. Fujimori, K. Ono, M. Kawasaki, and H. Koinuma, *Appl. Phys. Lett.* **87**, 162508 (2005).
- ⁷G. Koster, B. L. Kropman, G. J. H. M. Rijnders, D. H. A. Blank, and H. Rogalla, *Appl. Phys. Lett.* **73**, 2920 (1998).
- ⁸G. Herranz, B. Martinez, J. Fontcuberta, F. Sánchez, M. V. Garcia-Cuenca, C. Ferrater, and M. Varela, *Appl. Phys. Lett.* **82**, 85 (2003).
- ⁹J. Choi, C. B. Eom, G. Rijnders, H. Rogalla, and D. H. A. Blank, *Appl. Phys. Lett.* **79**, 1447 (2001).
- ¹⁰See S. D. Bader, *J. Magn. Magn. Mater.* **100**, 440 (1991).
- ¹¹Jing Xia, P. T. Beyersdorf, M. M. Fejer, and A. Kapitulnik, *Appl. Phys. Lett.* **89**, 062508 (2006).
- ¹²Jing Xia, Y. Maeno, P. T. Beyersdorf, M. M. Fejer, and A. Kapitulnik, *Phys. Rev. Lett.* **97**, 167002 (2006).
- ¹³For a recent review, see, e.g., J. Nogués and I. K. Schuller, *J. Magn. Magn. Mater.* **192**, 203 (1999).
- ¹⁴Below 9 ML, a step structure in the hysteresis is occasionally observed, presumably due to a competition between domain wall and coherent reversal of domains: see, e.g., R. A. Hyman, A. Zangwill, and M. D. Stiles, *Phys. Rev. B* **58**, 9276 (1998).
- ¹⁵O. Riss, A. Tsukernik, M. Karpovsky, and A. Gerber, *J. Magn. Magn. Mater.* **298**, 73 (2006).
- ¹⁶L. Klein, J. S. Dodge, T. H. Geballe, A. Kapitulnik, A. F. Marshall, L. Antognazza, and K. Char, *Appl. Phys. Lett.* **66**, 2427 (1995).
- ¹⁷G. Herranz, N. Dix, F. Sánchez, B. Martinez, J. Fontcuberta, M. V. Garcia-Cuenca, C. Ferrater, M. Varela, D. Hrabovskyy, and A. R. Fert, *J. Appl. Phys.* **97**, 10M321 (2005).
- ¹⁸J. M. Rondinelli, N. M. Caffrey, S. Sanvito, and N. A. Spaldin, *Phys. Rev. B* **78**, 155107 (2008).
- ¹⁹P. Mahadevan, F. Aryasetiawan, A. Janotti, and T. Sasaki, arXiv:0812.2098 (unpublished).
- ²⁰I. I. Mazin and D. J. Singh, *Phys. Rev. B* **56**, 2556 (1997).